

A software framework for pipelined arithmetic algorithms in field programmable gate arrays

J. B. Kim and E. Won*

Physics department, Korea University, Anam-ro 145, Seongbuk-gu, 02841 Seoul, Korea

Abstract

Pipelined algorithms implemented in field programmable gate arrays are extensively used for hardware triggers in the modern experimental high energy physics field and the complexity of such algorithms increases rapidly. For development of such hardware triggers, algorithms are developed in C++, ported to hardware description language for synthesizing firmware, and then ported back to C++ for simulating the firmware response down to the single bit level. We present a C++ software framework which automatically simulates and generates hardware description language code for pipelined arithmetic algorithms.

Keywords: Software framework, FPGA, Pipelined arithmetic algorithms, VHDL, C++, code generation

1. Introduction

In the modern experimental high energy physics field, detectors with massive number of channels are used to identify physical processes that occur when colliding particles. Because the rate of colliding particles including uninteresting background are in the scale of MHz [1, 2, 3] and data readout from detectors are in the scale of megabytes [4, 5, 6], it is currently impossible to record all the collision data which would be produced in the terabyte per second scale. Therefore a hardware trigger which determines whether the data should be recorded or not is required. The trigger should filter the detector data in such a way that only the physics processes of interest are written to a permanent storage at an acceptable rate. The trigger response also needs to be prompt in making the decision, because each sub-detector can hold its data for only a limited amount of time due to hardware limits which is in the scale of micro seconds [1, 7, 8]. The trigger should perform all of its logic before this limited amount of time is reached.

Field programmable gate arrays (FPGAs) are integrated circuits that are programmed using hardware description language. Due to their programmable and parallel nature, they have been used for event triggers in the modern experimental high energy physics field [9, 10, 11] extensively. FPGA based trigger algorithms generally use integer based calculations [10, 12, 13, 14]. Although floating-point calculation can be implemented in FPGAs, the calculation latency, FPGA resource usage are significantly higher as discussed in Ref. [15, 16].

On the other hand, physics related data are generally handled using floating-point calculations with general purpose computers and physics analysis software are built with floating-point calculations for precise results. One needs to use these software to study the performance of trigger algorithms. The implemented trigger should also be simulated in these software in such way that the effects of the trigger on the recorded physics of interest can be studied, as well as to be compared with the output from the real hardware down to the single bit level.

Due to these facts, trigger algorithms are usually developed in two software versions. One that uses floating-point calculations and one that uses integer calculations [10, 12, 13, 14]. The floating-point version shows the pure algorithm performance while the integer version shows the degradation of performance due to the constraints of integer calculation and the performance of the FPGA algorithms. Due to the coexistence of the two versions, one constantly needs to synchronize them when the algorithms are modified in one of the versions. To make matters worse, FPGAs are programmed using a hardware description language so that there can even be three versions of the same algorithm that are not necessarily developed by one individual. These various versions make the maintenance of the level one trigger software extremely difficult. A solution to these problems could be to use high level synthesis (HLS) packages such as Vivado HLS [17]. One can write code in C++ and let HLS convert it into a hardware description language. If latency or resources of a FPGA is not an issue, this would be the best solution. However, as discussed earlier, floating-point calculation implemented in FPGAs take up much more latency and resources, which is also a concern for Vivado HLS [18]. Integer or fixed-point algorithms can be written in C++ using the classes

*Corresponding author

Email address: eunil@hep.korea.ac.kr (E. Won)

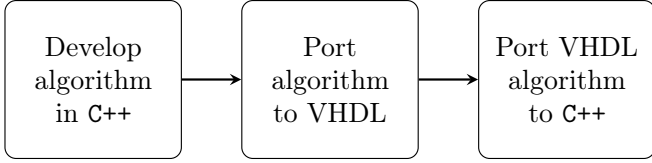


Figure 1: A development procedure for firmware algorithms. An algorithm is developed with floating-point based calculations using simulated data as input. It is then ported to VHDL with integer based calculations to synthesize firmware for a given FPGA. To study the performance of the synthesized firmware, it is ported back to software which simulates the firmware response exactly bit-by-bit.

provided by Vivado HLS, but then the precision and bit widths for each calculation should to be additionally considered. Also there would still be the issue of maintaining two versions, floating-point and fixed-point, of the same algorithm.

We have developed a framework that solves the multiple version problem which uses integer based calculations for the hardware description language. Once an algorithm is implemented in the framework, one can obtain the floating-point calculation result, integer calculation result, and very high speed integrated circuit hardware description language (VHDL) code simultaneously.

In this work, a framework for pipelined arithmetic algorithms in FPGAs is reported. The goals and design of the framework are explained. The three C++ classes that were developed for the framework are described. Algorithms that were developed using this framework are discussed as examples. We also compare between our framework and Vivado HLS for a linear regression algorithm.

2. Goals

A typical procedure of firmware algorithm development is shown in Fig. 1. Algorithms are developed and tested in C++ first. After the algorithms are validated they are ported to hardware description language such as VHDL. There are several issues that should be considered when porting to VHDL. Floating-point numbers should be converted to integers. The bit width of all variables should be determined. Division and non-linear operators such as trigonometric operators should be implemented using look-up tables (LUTs). The inputs to an operator should be properly buffered so that the clock cycle between them are in synchronization. Overflow and underflow should be prevented when doing addition, subtraction, and multiplication. In order to limit the FPGA resource usage, the bit width of the inputs to the multiplication operator should be small enough to be implemented in a digital signal processing (DSP) slice [19]. After porting to VHDL, the resources used by the algorithm should be small enough to fit in to the chosen target FPGA. One way to reduce the resource is by controlling the bit widths for the LUTs. Due to the loss of calculation precision when porting, the VHDL codes need to be simulated, a priori to confirm if

they can achieve their goals. A floating-point calculation of the algorithm should be performed to confirm the loss of precision due to this integer conversion. The VHDL codes should be simulated in C++ in such a way that the results can be used in studying other algorithms. Simulation in C++ will also help in debugging the firmware algorithm most efficiently.

A framework is developed to simplify the entire process of pipelined arithmetic firmware algorithm development. The framework can execute the algorithm using floating-point calculations, simulate the integer-valued version of the algorithm, automatically generate VHDL code, and deal with all the issues described previously on arithmetic algorithms. After an algorithm is developed, the framework will handle the rest of the development process most efficiently.

3. Design

Three classes have been developed in total. The first one is for simulating VHDL signals and the second one is for LUTs that use block random access memories (BRAMs) [20]. The third class is to store the information related with our VHDL codes. Clock cycles are taken into consideration so that the signals are properly buffered for the pipelined algorithms in the VHDL code.

3.1. Signal class

The signal class has been implemented to simulate the signed and unsigned VHDL types. Since algorithms generally use floating-point variables but VHDL signals are integer variables, a conversion from floating-point values to integer values are executed when the range of the floating-point variables and bit widths are given. For signed variables, the conversion is done by the following equations

$$\text{symmetric max} = \max(\text{maximum float value}, \text{minimum float value}) \quad (1)$$

$$\text{conversion constant} = \frac{2^{(n-1)} - 0.5}{\text{symmetric max}} \quad (2)$$

$$\text{integer variable} = \lfloor \text{float variable} \times \text{conversion constant} \rfloor, \quad (3)$$

where n is a given the bit width, \max is the maximum function, $\lfloor \rfloor$ is a round-off function, and float refers to a floating-point. For unsigned variables, the conversion is done by the following equation

$$\text{conversion constant} = \frac{2^n - 0.5}{\text{maximum float value}} \quad (4)$$

$$\text{integer variable} = \lfloor \text{float variable} \times \text{conversion constant} \rfloor, \quad (5)$$

where n is a given bit width. The real value which the integer value represents can be calculated using following

equation

$$\text{real value} = \frac{\text{integer value}}{\text{conversion constant}}. \quad (6)$$

Addition, subtraction and multiplication operators have been implemented as class methods. The maximum and minimum values are calculated and stored in the class so that bit widths can be reduced to a minimum for each operator. Before adding and subtracting, the input’s conversion constants should be matched. They are similarly matched by multiplying a factor of two which is done by bit shifting. The multiplication method is implemented so that only one DSP slice is used to reduce FPGA resources. One DSP slice can perform 25 bit \times 18 bit calculations so that the bit width of the input is constrained to 25 bits or 18 bits by applying bit shifts. An if-else method is also implemented to be able to control the flow of the algorithm. It consists of a comparing component and an assigning component. Two signals can be compared with a compare method which receives ==, !=, >=, >, <=, <, &&, and || as an argument and returns a Boolean type signal. Depending on the comparison, different arithmetic operations can be preformed by setting the assigning component.

Each method for this class has logic which can generate VHDL code. To reduce calculation overhead, a flag is used to turn it on and off. All the methods also perform floating-point calculations where the results are stored in the class so that it can be compared with the integer-valued calculations.

The <= operator is overloaded to represent that the logic should be performed in one clock cycle as in VHDL. When this operator is used, the clock cycle of the signal in the left-hand side will be assigned with one addition clock cycle compared to the right-hand side.

An example C++ code for pipelined addition using the framework is shown in Listing 1. After two ϕ values are added together in one clock cycle, another ϕ value is added to the sum in the next clock cycle, as shown in the bottom part of Listing 1. The automatically generated VHDL code is shown in Listing 2. The signals are defined according to the logic in the implemented C++ code. The buffers required for pipelining the logic are also defined. Sequential VHDL statements are written according to the C++ code. The framework simulated results is shown in Table 1. The simulated floating-point values, integer values and real values for each signal are shown. It demonstrates that the framework simulation is working well.

Listing 1: Example C++ code for a pipelined addition. The <= operator is overloaded to represent the logic should be performed in one clock cycle. `phi_0`, `phi_1`, and `phi_2` are defined as signed signals with 10 bits and have a range from -3.14 to 3.14. `phi_0`, `phi_1`, and `phi_2`’s current values are 1.57, -0.785, and 0.785. `phi_0` and `phi_1` are added during one clock cycle to obtain `phiAdd`. This is added with `phi_2` to obtain `phiAdd2` on the next clock cycle.

```
// Define signals
JSIGNAL phi_0 <= JSIGNAL(10, 1.57, -3.14, 3.14, 0,
storage);
```

```
JSIGNAL phi_1 <= JSIGNAL(10, -0.785, -3.14, 3.14, 0,
storage);
JSIGNAL phi_2 <= JSIGNAL(10, 0.785, -3.14, 3.14, 0,
storage);
// Addition
JSIGNAL phiAdd <= phi_0 + phi_1;
// Pipelined addition
JSIGNAL phiAdd2 <= phiAdd + phi_2;
```

Listing 2: Automatically generated VHDL for a pipelined addition example. The framework defines the signals according to the JSIGNAL properties in the C++ code. There is also a buffer for `phi_2` to synchronize the clock cycle between `phiAdd` and `phi_2` when calculating `phiAdd2`. The framework writes VHDL according to the logic defined in C++.

```
-- Define signals
signal phi_0 : signed(9 downto 0) := (others=>'0');
signal phi_1 : signed(9 downto 0) := (others=>'0');
signal phiAdd : signed(10 downto 0) := (others=>'0');
signal phiAdd2 : signed(11 downto 0) := (others=>'0');
type S10D1Array is array(0 downto 0) of signed(9 downto 0);
signal phi_2_b : S10D1Array := (others=>(others=>'0'));

-- Sequential logic
phiAdd <= resize(phi_0,11)+phi_1;
phiAdd2 <= resize(phiAdd,12)+phi_2_b(0);
phi_2_b(0) <= phi_2;
```

Name	Float value	Integer value	Real value
<code>phi_0</code>	1.570	256	1.57153
<code>phi_1</code>	-0.785	-128	-0.78577
<code>phi_2</code>	0.785	128	0.78577
<code>phiAdd</code>	0.785	128	0.78577
<code>phiAdd2</code>	1.570	256	1.57153

Table 1: Results of the pipelined addition example, where float value is the floating-point value, integer value is the converted integer value from the floating-point value, and real value is the value that the integer value represents. Difference between the floating-point values and integer representation values are due to the conversion from floating-point values to integer values.

3.2. LUT class

The LUT class generates LUTs with signal instances as input and output which can be used for operations that are not directly possible in VHDL. Division and trigonometric operators can be implemented using this class. The LUTs are implemented using BRAMs. After the LUT class is properly set, it can generate a text file which has all the values to be stored in the BRAM. This text file¹ is then used with a commercial synthesis tool [21]. The input is transformed so that its minimum value is zero which reduces the BRAM size in certain cases. The output of the BRAM also shares this property. A constant value is added to get the proper output. Although this process uses a few clock cycles, it can drastically reduce the BRAM size in certain cases. This class generates VHDL code which should be used with a Block Memory Generator IPCORE [21] and the generated text file.

¹This text file is called COE (coefficient file) within the Xilinx tools.

3.3. VHDL code storage class

This class stores the entire VHDL generated by the signal class and LUT class, so that the pipelined arithmetic algorithm can be written to a VHDL file. Also VHDL syntax for design entities, signal declaration, and buffers can be optionally added when generating the VHDL file.

4. Implementation examples

The Belle II experiment [1] aims to study the charge-conjugation and the parity violation in B or D meson system precisely and search for new physics at the SuperKEKB accelerator [22]. Due to the high beam current and small cross section of physics in interest, a fast and highly efficient trigger is required.

The level one trigger is implemented using FPGAs to achieve the above goals. It consists of several systems, and one of the major systems is the level one central drift chamber (CDC) trigger. The level one CDC trigger algorithms are implemented on merger boards [23] and third generation universal trigger boards (UT3), which are 6U VME [24] boards with optical cables. The UT3 board was developed by the high energy accelerator research organization (KEK) for the Belle II level one trigger. The structure and connections between the CDC front-end, merger, track segment finder, 2D tracker, 3D tracker and neural network tracker boards can be seen in Fig. 2, where all connections between the boards are with optical cables. These UT3 boards which are used for most of the algorithms in the level one CDC trigger, has a Virtex 6 HXT FPGA with 40 GTX and 24 GTH gigabit optical transceivers which can be seen in Fig. 3.

The level one trigger uses pipelined algorithms to find patterns potentially originated from physics of interest. The pipelined algorithms finds track parameters obtained from the CDC hit information and minimize χ^2 for the track parameter fits. They also include logic for combining CDC track parameters with electromagnetic calorimeter (ECL) cluster parameters. Our framework described above has been used to develop the firmware and C++ code for the simulation in order to implement these algorithms automatically. All the algorithms in the following sections are implemented on the UT3 boards.

4.1. χ^2 minimization fitters

There are two fitters that have been developed using our framework. One fitter minimizes χ^2 defined as

$$\chi^2 = \sum_i^5 \frac{[2(a \cos \phi_i + b \sin \phi_i) - r_i]^2}{\sigma_i^2}, \quad (7)$$

where a and b are fit parameters and ϕ_i , r_i and σ_i are input variables related with charged tracks in CDC. The second fitter transforms the wire hit information into a geometric representation and minimizes a χ^2 to obtain track

parameters. The transformation equations are

$$\phi_{\text{fineSt}} = \phi_{\text{st}} \pm \text{LUT}(\text{TDC} - t_0) \quad (8)$$

$$\phi_{\text{ax}} = \pm \cos^{-1} \left(\frac{r\rho}{2} \right) + \phi_{\text{incident}} \mp \frac{\pi}{2} \quad (9)$$

$$z = \frac{z_{\text{endplate}} - 2r \sin \left(\frac{\phi_{\text{fineSt}} - \phi_{\text{ax}}}{2} \right)}{\tan \theta_{\text{st}}} \quad (10)$$

$$s = \sin^{-1} \left(\frac{r\rho}{2} \right), \quad (11)$$

where ϕ_{fineSt} is the fine phi position of a hit stereo wire (wires that have a finite phi shift at the end plates), ϕ_{st} is the phi position of a hit stereo wire, TDC is the wire hit time relative to the revolution of the beam, t_0 is the event time relative to the revolution of the beam, LUT is a look up table that has the x-t curve of the CDC, ϕ_{ax} is the phi position if a stereo wire is an axial wire (wires that are parallel to the beam), r is the radius of a stereo wire layer, ρ is the curvature of a track, ϕ_{incident} is the incident angle of a track, z is the geometric hit position, z_{endplate} is the distance from the IP to the end plate of the CDC, and s is the arc length of the track in a two dimensional plane for a stereo wire layer [25]. The χ^2 is defined as

$$\chi^2 = \sum_i^4 \frac{[(\cot \theta \times s_i + z_0) - z_i]^2}{\sigma_i^2}, \quad (12)$$

where $\cot \theta$ and z_0 are fit parameters, z_i and s_i are the z and s for hit stereo wires, and σ_i is the resolution of z_i . There are analytical solutions to these χ^2 minimization which have been used to calculate the fit parameters. They are

$$a = \frac{\sum_i^5 \frac{\sin^2 \phi_i}{\sigma_i^2} \sum_i^5 \frac{r_i \cos \phi_i}{\sigma_i^2} - \sum_i^5 \frac{\sin \phi_i \cos \phi_i}{\sigma_i^2} \sum_i^5 \frac{r_i \sin \phi_i}{\sigma_i^2}}{2 \left[5 \sum_i^5 \frac{\cos^2 \phi_i}{\sigma_i^2} \sum_i^5 \frac{\sin^2 \phi_i}{\sigma_i^2} - \left(\sum_i^5 \frac{\sin \phi_i \cos \phi_i}{\sigma_i^2} \right)^2 \right]} \quad (13)$$

$$b = \frac{\sum_i^5 \frac{\cos^2 \phi_i}{\sigma_i^2} \sum_i^5 \frac{r_i \sin \phi_i}{\sigma_i^2} - \sum_i^5 \frac{\sin \phi_i \cos \phi_i}{\sigma_i^2} \sum_i^5 \frac{r_i \cos \phi_i}{\sigma_i^2}}{2 \left[5 \sum_i^5 \frac{\cos^2 \phi_i}{\sigma_i^2} \sum_i^5 \frac{\sin^2 \phi_i}{\sigma_i^2} - \left(\sum_i^5 \frac{\sin \phi_i \cos \phi_i}{\sigma_i^2} \right)^2 \right]} \quad (14)$$

and

$$\cot \theta = \frac{\sum_i^4 \frac{1}{\sigma_i^2} \sum_i^4 \frac{s_i z_i}{\sigma_i^2} - \sum_i^4 \frac{s_i}{\sigma_i^2} \sum_i^4 \frac{z_i}{\sigma_i^2}}{\sum_i^4 \frac{1}{\sigma_i^2} \sum_i^4 \frac{s_i^2}{\sigma_i^2} - \left(\sum_i^4 \frac{s_i}{\sigma_i^2} \right)^2} \quad (15)$$

$$z_0 = \frac{-\sum_i^4 \frac{s_i}{\sigma_i^2} \sum_i^4 \frac{s_i z_i}{\sigma_i^2} + \sum_i^4 \frac{s_i^2}{\sigma_i^2} \sum_i^4 \frac{z_i}{\sigma_i^2}}{\sum_i^4 \frac{1}{\sigma_i^2} \sum_i^4 \frac{s_i^2}{\sigma_i^2} - \left(\sum_i^4 \frac{s_i}{\sigma_i^2} \right)^2}. \quad (16)$$

These solutions consist of addition, subtraction, multiplication, division and trigonometric operations. Division

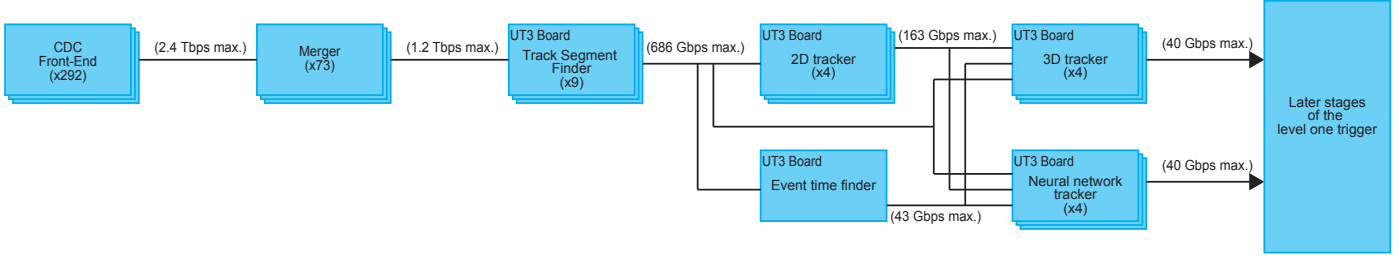


Figure 2: Structure of the Belle II level one CDC trigger. The level one CDC trigger consists (from the left) of CDC front-end boards, merger boards, track segment finder boards, 2D tracker boards, event time finder board, 3D tracker boards and neural network boards. Data is transferred using gigabit optical transceivers between boards. The CDC front-end boards receive the CDC detector response. The merger boards combine the CDC front-end data. The track segment finder finds partial tracks. The 2D tracker find tracks in a two dimensional plane. The event time finder finds the initial timing of the event. The 3D tracker and neural network tracker find three dimensions tracks.

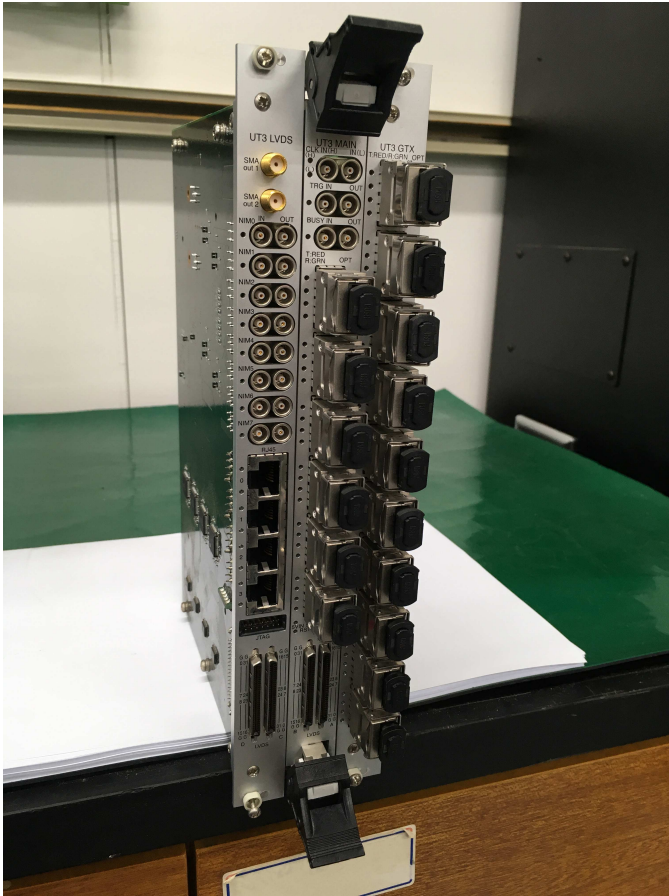


Figure 3: A picture of the UT3 board. The UT3 board is a 6U VME board with two daughter boards that extend the number of channels of communication. It has a Vertex 6 HXT FPGA with 40 GTX and 24 GTH gigabit optical transceivers. It was developed by the high energy accelerator research organization (KEK) for the Belle II level one trigger.

and trigonometric operations are implemented using LUT class.

For the second fitter, we used the VHDL code from our framework to generate firmware. Xilinx ISE [26] was used to generate the firmware for the FPGA on the UT3 board where the clock frequency time constraint was set to 127 MHz. Xilinx ISE reported that 2,365 slice registers, 2,919 slice LUTs, 18 RAMB36E1s, 5 RAMB18E1s, and 52 DSP48E1s were used for the design and that all timing constraints were met. A firmware based test bench was developed to record the results from the firmware module that has the generated VHDL code. We compare the firmware results with the simulated results from our framework.

The structure of the firmware based test bench can be seen in Fig. 4. The firmware based test bench has LUTs which contain values that are acquired from a trigger simulation (TSIM). The values are given to the firmware module clock by clock. The output of the firmware module is connected to Chipscope [27] to record the firmware response which is shown in Fig. 5. The values between the recorded the firmware results and simulation results from the framework are found to be identical down to single bit level. In Fig. 6, a large statistics of the integer output of the framework and recorded firmware results for z_0 are shown to be exactly the same. We were also able to confirm that the firmware latency is 19 clock cycles which was the expected value from the framework. The recorded firmware results and the float-point calculation results from the framework for z_0 have a strong correlation which is shown in Fig. 7. To see the precision of the recorded firmware results, they are multiplied with a conversion constant and then subtracted with the float-point calculation results from the framework where a histogram of z_0 precision is shown in Fig. 8. The histogram's root mean square (RMS) was found to be 0.2 cm which is below the expected resolution from the z_0 fitter algorithm of $\mathcal{O}(1)$ cm [25]. These results show that our framework works well and satisfy the level 1 trigger requirements of Belle II.

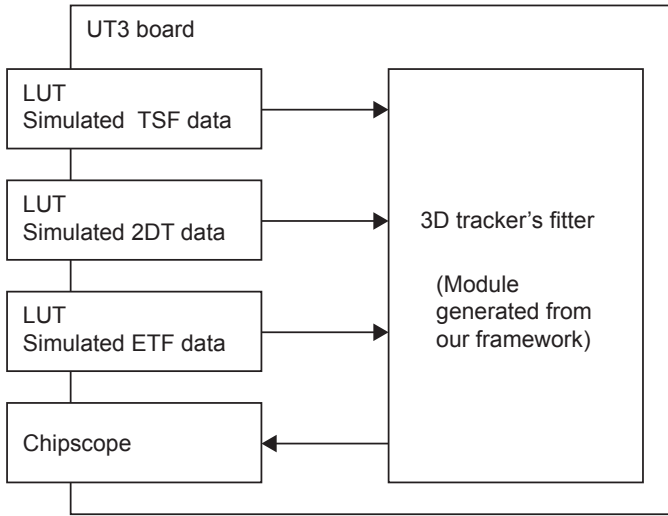


Figure 4: Firmware based test bench structure for testing the 3D tracker's fitter firmware module which was generated from the framework. The firmware module is tested with data from a TSIM which are held in LUTs. The LUTs contain tracks segment finder (TSF), 2D tracker (2DT), and event time finder (ETF) data. Chipscope is connected to record the output of the firmware.

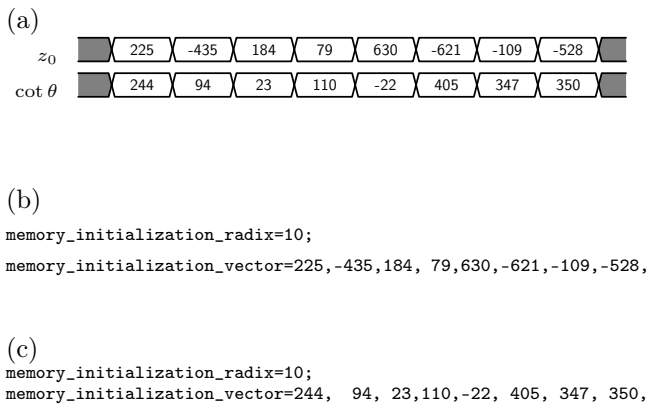


Figure 5: Recorded results of the firmware using Chipscope and integer based simulation results from the framework for an automatically generated VHDL code. In (a), recorded firmware results for z_0 and $\cot \theta$ are shown. In (b), integer based simulation results from the framework for z_0 are shown. In (c), integer based simulation results from the framework for $\cot \theta$ are shown. The firmware results and integer based simulation results from the framework match perfectly.

Framework sim. vs Firmware

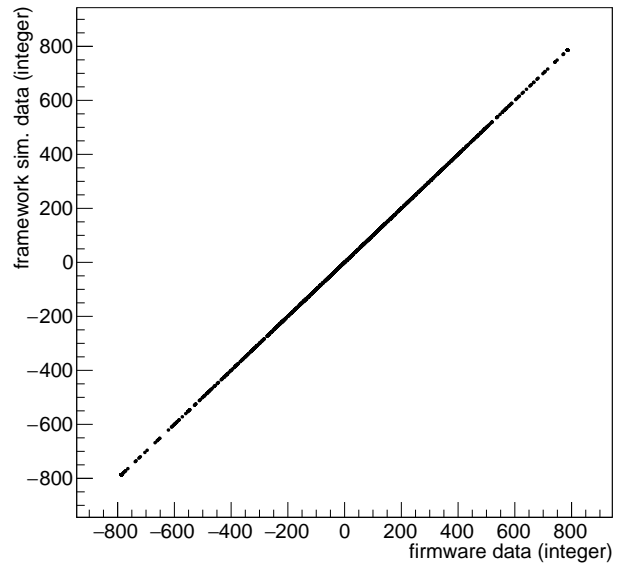


Figure 6: Comparison of z_0 between the recorded firmware results and the integer based simulation results from the framework (framework sim.) for an automatically generated VHDL code. The results are exactly equal.

Floating-point vs Firmware

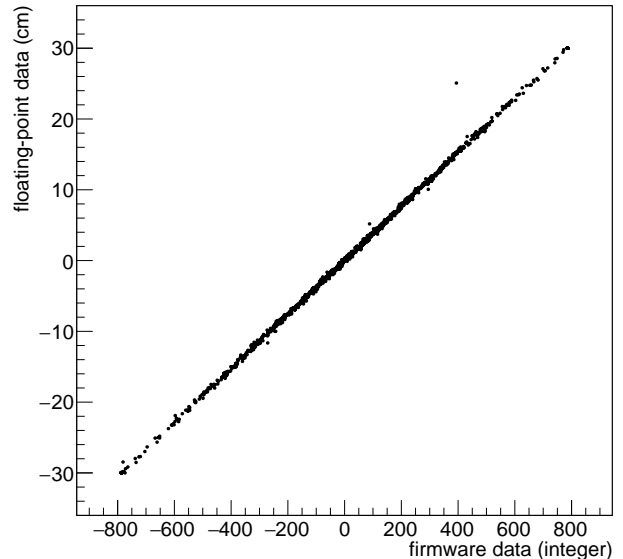


Figure 7: Correlation of z_0 between the recorded firmware results and the floating-point calculation results. They have a strong correlation with each other. The outliers are due to the accumulation of lost precision when processing the pipelined integer based algorithm.

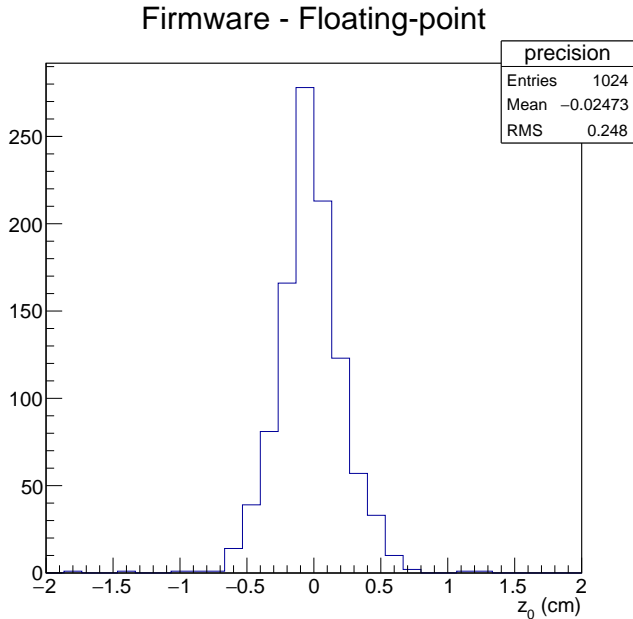


Figure 8: Histogram of the firmware precision for z_0 . A conversion constant was multiplied to the recorded firmware results and subtracted with the float-point calculated results to calculate the precision. The RMS is 0.2 cm which is below the expected resolution from the z_0 fitter algorithm of $\mathcal{O}(1)$ cm [25].

4.2. CDC geometry calculation

By using track parameters, the position of the track at a specific layer of the CDC is required to be calculated. The position is calculated in two steps. In the first step, our algorithm calculates the ϕ_{ax} position of the track for the layer of the CDC using Eq. 9. The second step converts the ϕ_{ax} position to a corresponding wire position at a given layer of interest. These calculations consist of addition, subtraction, multiplication and trigonometric operations. The trigonometric operations were implemented using the LUT class. A firmware test bench confirmed that the synthesized firmware and simulated algorithm using the framework return the same results.

4.3. Combining CDC track and ECL cluster parameters

The framework has been used in algorithms that combines CDC trigger and ECL trigger information. The level one CDC trigger outputs track momentum parameters while the level one ECL trigger outputs cluster positions created by the deposited energy from the tracks. The two information can be combined using the position of the track which can increase the performance of the trigger. Using the track momentum parameters from the CDC trigger, the expected position of the track in the ECL detector is calculated which is used to calculate distance between the expected position and the actual cluster position. This distance can be used to relate the CDC tracks and ECL clusters. The ratio between energy and momentum of the track is also calculated which can help to identify the par-

Linear regression	float HLS	fixed HLS	framework
LUT	8061	1104	723
FF	8064	501	283
BRAM	0	5	2.5
DSP	126	40	29
Latency (clocks)	33	5	5
z_0 precision (cm)		0.12	0.13

Table 2: Comparison between HLS and the framework for a linear regression algorithm. A floating-point calculation (float HLS) and fixed-point calculation (fixed HLS) version was developed. The resource usage, latency, and precision are compared, where LUT are slice look-up tables, FF are flip-flops, BRAM are block RAMs, DSP are DSP slices, latency are the number of clock cycles to perform the algorithm, and z_0 precision is the RMS of a histogram where the results are subtracted with floating-point calculation results.

title. All of these calculations are implemented using the developed framework.

5. Comparison with Vivado HLS

Our framework was compared with Vivado HLS for a linear regression algorithm (Eq. 15 and Eq. 16). Floating-point and fixed-point versions were developed using Vivado HLS. For a fair comparison (latency wise), a LUT that replaces the division operator was also developed for the Vivado HLS fixed-point version case. All firmware were synthesized and implemented using the Vivado design suite [28]. The target FPGA and clock frequency timing constraint were set to xcvu080-ffvb2104-2-e and 127 MHz. Simulation results from Vivado HLS and our framework were used to measure the precision of the firmware where the input data is from TSIM. The precision is measured by filling a histogram with simulated firmware results subtracted by floating-point calculated results. We define the precision to be the RMS of the histogram. The resource usage, latency and precision can be found in Table. 2. We find that within the expected resolution from the z_0 fitter algorithm of $\mathcal{O}(1)$ cm, that our framework uses the least resources and latency, as demonstrated clearly in Table. 2.

6. Conclusions

A framework that allows automatic generation of pipelined algorithms in VHDL is implemented which also simulate the algorithms. It was validated with χ^2 minimization, a sub-detector geometry calculation, and combining algorithms of sub-detectors. It was compared with Vivado HLS and our framework is found to be more efficient resource and latency wise. Development and maintenance of pipelined arithmetic firmware algorithms using this framework is applied to a variety of situations and is demonstrated that the framework we developed is most efficient in dealing with these tasks. Our framework can be used for future trigger development in an efficient way.

Acknowledgment

We acknowledge support from the National Research Foundation of Korean Grants No. NRF-2017R1A2B3001968.

References

- [1] T. Abe, et al., Belle II Technical Design Report [arXiv:1011.0352v1](https://arxiv.org/abs/1011.0352v1).
- [2] Pamela Klabbers, Operation and Performance of the CMS Level-1 Trigger during 7 TeV Collisions, Physics Procedia 37 (Supplement C) (2012) 1908 – 1916, proceedings of the 2nd International Conference on Technology and Instrumentation in Particle Physics (TIPP 2011).
- [3] Imma Riu and the ATLAS Collaboration, Performance of the ATLAS Trigger with Proton Collisions at the LHC, Journal of Physics: Conference Series 331 (3) (2011) 032027.
- [4] R. Itoh, T. Higuchi, M. Nakao, S. Y. Suzuki, and S. Lee, Data Flow and High Level Trigger of Belle II DAQ System, IEEE Transactions on Nuclear Science 60 (5) (2013) 3720–3724.
- [5] G Bauer, et al., The data-acquisition system of the CMS experiment at the LHC, Journal of Physics: Conference Series 331 (2) (2011) 022021.
- [6] The ATLAS TDAQ Collaboration, The ATLAS Data Acquisition and High Level Trigger system, Journal of Instrumentation 11 (06) (2016) P06008.
- [7] C Foudas, The CMS Level-1 Trigger at LHC and Super-LHC.
- [8] P. B. Amaral, et al., The ATLAS Level-1 trigger timing setup, in: 14th IEEE-NPSS Real Time Conference, 2005., 2005, pp. 4 pp.–.
- [9] Y. Iwasaki, B. Cheon, E. Won, and G. Varner, Level 1 trigger system for the Belle II experiment, in: 2010 17th IEEE-NPSS Real Time Conference, 2010, pp. 1–9.
- [10] J Chaves, Implementation of FPGA-based level-1 tracking at CMS for the HL-LHC, Journal of Instrumentation 9 (10) (2014) C10038.
- [11] R. Caputo, et al., Upgrade of the ATLAS Level-1 trigger with an FPGA based Topological Processor, in: 2013 IEEE Nuclear Science Symposium and Medical Imaging Conference (2013 NSS/MIC), 2013, pp. 1–5.
- [12] E. Won, A hardware implementation of artificial neural networks using field programmable gate arrays, Nuclear Instruments and Methods in Physics Research Section A: Accelerators, Spectrometers, Detectors and Associated Equipment 581 (3) (2007) 816 – 820.
- [13] E. Bartz, et al., Fpga-based real-time charged particle trajectory reconstruction at the large hadron collider, in: 2017 IEEE 25th Annual International Symposium on Field-Programmable Custom Computing Machines (FCCM), 2017, pp. 64–71.
- [14] J. Wu, M. Wang, E. Gottschalk, and Z. Shi, Fpga curved track fitters and a multiplierless fitter scheme, IEEE Transactions on Nuclear Science 55 (3) (2008) 1791–1797.
- [15] N. Shirazi, A. Walters, and P. Athanas, Quantitative analysis of floating point arithmetic on fpga based custom computing machines, in: Proceedings IEEE Symposium on FPGAs for Custom Computing Machines, 1995, pp. 155–162.
- [16] W. B. Ligon, et al., A re-evaluation of the practicality of floating-point operations on fpgas, in: Proceedings. IEEE Symposium on FPGAs for Custom Computing Machines (Cat. No.98TB100251), 1998, pp. 206–215.
- [17] Xilinx, Vivado Design Suite User Guide: High Level Synthesis, available at https://www.xilinx.com/support/documentation/sw_manuals/xilinx2014_1/ug902-vivado-high-level-synthesis.pdf.
- [18] Xilinx, Reduce Power and Cost by Converting from Floating Point to Fixed Point, available at https://www.xilinx.com/support/documentation/white_papers/wp491-floating-to-fixed-point.pdf.
- [19] Xilinx, Virtex-6 FPGA DSP48E1 Slice, available at https://www.xilinx.com/support/documentation/user_guides/ug369.pdf.
- [20] Xilinx, Virtex-6 FPGA Memory Resources, available at https://www.xilinx.com/support/documentation/user_guides/ug363.pdf.
- [21] Xilinx, LogiCORE IP Block Memory Generator, available at https://www.xilinx.com/support/documentation/ip_documentation/blk_mem_gen/v7_3/pg058-blk-mem-gen.pdf.
- [22] Yukiyoishi Ohnishi, et al., Accelerator design at SuperKEKB, Progress of Theoretical and Experimental Physics 2013 (3) (2013) 03A011.
- [23] Y. S. Teng, et al., The status of high-speed trigger multiplexer module with aurora protocol implemented on arria ii fpga for the belle ii cylindrical drift chamber detector, in: 2013 IEEE Nuclear Science Symposium and Medical Imaging Conference (2013 NSS/MIC), 2013, pp. 1–3. doi:10.1109/NSSMIC.2013.6829748.
- [24] IEEE Standard for a Versatile Backplane Bus: VMEbus, ANSI/IEEE Std 1014-1987 doi:10.1109/IEEESTD.1987.101857.
- [25] E. Won, J. B. Kim, and B. R. Ko, Three dimensional fast tracker for central drift chamber based level 1 trigger system in the Belle II experiment [arXiv:1711.02800v1](https://arxiv.org/abs/1711.02800v1).
- [26] Xilinx, ISE Design Suite 14, available at https://www.xilinx.com/support/documentation/sw_manuals/xilinx14_7/irn.pdf.
- [27] Xilinx, Chipscope Pro Software and Cores, available at https://www.xilinx.com/support/documentation/sw_manuals/xilinx14_7/chipscope_pro_sw_cores_ug029.pdf.
- [28] Xilinx, Vivado Design Suite User Guide, available at https://www.xilinx.com/support/documentation/sw_manuals/xilinx2016_4/ug893-vivado-ide.pdf.